Geophysical Research Letters

RESEARCH LETTER
10.1029/2021GL097022

Changes in Mechanisms and Characteristics of Western U.S. Floods Over the Last Sixty Years

Huilin Huang[1], Michael R. Fischella[1], Yufei Liu[2], Zhaoxin Ban[1], Jessica V. Fayne[1], Dongyue Li[1,2], Kyle C. Cavanaugh[1], and Dennis P. Lettenmaier[1,2]

[1]Department of Geography, University of California, Los Angeles, CA, USA, [2]Department of Civil and Environmental Engineering, University of California, Los Angeles, CA, USA

Key Points:

- The frequency and magnitude of rain-on-snow floods have decreased across the western U.S., and snowmelt floods are occurring earlier
- Floods generated by convective storms (primarily in the Southwest) have increased in frequency and magnitude
- Except for the above-mentioned changes, the frequency, magnitude, and timing of floods have been relatively stable over time

Supporting Information:

Supporting Information may be found in the online version of this article.

Correspondence to:

D. P. Lettenmaier,
dlettenm@ucla.edu

Citation:

Huang, H., Fischella, M. R., Liu, Y., Ban, Z., Fayne, J. V., Li, D., et al. (2022). Changes in mechanisms and characteristics of western U.S. floods over the last sixty years. *Geophysical Research Letters*, *49*, e2021GL097022. https://doi.org/10.1029/2021GL097022

Received 15 NOV 2021
Accepted 18 JAN 2022

Abstract Climate change is linked to changing precipitation, yet uncertainty remains as to whether and how hydroclimatic changes will influence flood frequency, magnitude, and timing. Part of this uncertainty is because few regional-scale studies have analyzed changes in floods produced by different mechanisms. We identify six flood generating mechanisms (FGMs) based on prominent meteorological processes and moisture supply to the soil column in the Western U.S.; these include large-scale frontal storms (atmospheric and non-atmospheric rivers), monsoons, convective storms, snowmelt, and rain-on-snow. We assess trends in the frequency, magnitude, and timing of floods produced by different FGMs across 119 basins during 1960–2018. Overall, we find decreased frequency and magnitude of rain-on-snow-driven floods, increased frequency and magnitude of convective-storm-driven floods, and a temporal shift to earlier in the year for snowmelt-driven floods. The flood characteristics are generally stable for floods produced by other FGMs.

Plain Language Summary Floods are among the most common and costliest of natural disasters. Extreme rainfall is a major cause of flooding and has become more common as global temperatures have increased. However, many studies show that the number and size of flood events remain mostly unchanged. It is possible that climate change is affecting different types of floods in different ways, and so we separate floods into different categories and evaluate trends on a category-by-category basis. In particular, we group floods across the western U.S. into six categories, which we term flood generating mechanisms (FGMs). These include rain-on-snow, snowmelt, monsoons, convective storms, and two types of frontal storms. We then separately describe trends in the frequency, magnitude, and timing for each FGM from 1960 to 2018. We find that floods generated by convective storms have become more common and more extreme. On the other hand, rain-on-snow floods have become rarer and less extreme. Also, floods caused by snowmelt are occurring earlier within the year. Most of the other categories do not show significant changes in flood characteristics. These results give us important information on the types of flooding that may be most impacted by future climate change, which can aid future flood planning efforts.

1. Introduction

In recent decades, floods have accounted for billions of dollars in economic damage and hundreds of lives lost annually in the U.S. (Downton et al., 2005). Therefore, it is of both scientific and public interest to understand how and why flood frequency, magnitude, and timing have changed in recent decades. Where flood changes have occurred, the causes may be either anthropogenic or natural (Berghuijs et al., 2014). For example, Blum et al. (2020) found that annual maximum flood magnitudes increased by 3.3%, on average, for each percentage point increase in impervious cover. Furthermore, climate change is increasing the intensity and variability of rainfall extremes globally (Donat et al., 2013; Huang et al., 2020; Kendon et al., 2014; Min et al., 2013; Wanders et al., 2017; Westra et al., 2013), which has the potential to increase flood frequency and magnitudes (Pall et al., 2011). Flood frequency analysis is a key tool for engineers and water resources managers who are charged with designing and managing resilient flood infrastructure (Fayne et al., 2019; Perez et al., 2021; Yan et al., 2020). Recent studies have pointed to deficiencies in flood infrastructure planning that is still mostly based on an assumption of stationary climate, and fails to account for non-stationary effects of diverse "mixed populations" in flood frequency analysis (Barth et al., 2017, 2018, 2019; Villarini et al., 2009). On the other hand, climate-driven changes in flooding have not been widely observed (Archfield et al., 2016; Do et al., 2017; Hall et al., 2014; Hodgkins et al., 2017; Lins & Slack, 1999), and in general, there is no consensus as to whether floods are changing in response to precipitation changes (Sharma et al., 2018). While there is an expectation,

based on the first principle, that flood dates in snow-affected river basins should shift earlier in the year (Bindoff et al., 2013), the later shift of flood timing is also observed in southern Australia and part of the Europe (Bloschl et al., 2017; Wasko et al., 2020).

A primary challenge in understanding how climate change impacts flood frequency, magnitude, and timing is posed by the complex interactions among the hydrometeorological and physiographic factors that affect floods (B Merz et al., 2012; Sharma et al., 2018). While various studies have shown that flood responses to climate change are ultimately determined by changes to their hydrometeorological drivers (such as extreme rainfall (Mass et al., 2011; Wasko & Sharma, 2015), snowmelt (Dettinger & Cayan, 1995), or rain-on-snow (Freudiger et al., 2014); these changes are caused by different meteorological processes. For example, convective rainfall, a major contributor to flash floods, is particularly sensitive to warming, as it is produced by the upward motion of warm moist air locally. Convective rainfall rates have been observed to increase by as much as 14% $°C^{-1}$, double the 7% $°C^{-1}$ increase in precipitable water expected from the Clausius–Clapeyron relation, due to increasing water vapor with temperature and enhanced latent heat release (Berg et al., 2013; Lenderink & Van Meijgaard, 2008). Contrastingly, large-scale rainfall events caused by atmospheric rivers (ARs) and monsoons are related to moisture transport from remote tropical oceans. ARs are found (and projected) to be more frequent and more extreme due to increased water vapor transport and thermal fluxes (Gershunov et al., 2017; Huang et al., 2020; Ralph et al., 2020). All these hydrometeorological drivers affect extreme rainfall and snow events and thus flooding in different ways.

While numerous studies have explored how rainfall and snow regime changes affect floods (Archfield et al., 2016; Do et al., 2017; Wasko et al., 2020; Wasko & Sharma, 2017), it is not well understood how changes in flood characteristics (frequency, magnitude, and timing) are linked to flood generating mechanisms. Previous hydrological research has generally focused on specific flood events, with area and event-specific characterization of hydrometeorological variables and physiographic factors (Bloschl et al., 2013; Ralph et al., 2006). Thus, it is difficult to apply the conclusions of these studies to other river basins or to make inferences at the regional scale. While a few studies have explored changes of certain types of floods throughout the conterminous United States (Barth et al., 2017; Davenport et al., 2020; Dethier et al., 2020; Dudley et al., 2017) there has to date not been a cohesive interpretation of how different meteorological and land surface processes produce floods at the regional scale, and over the W-US in particular. Recently, some studies have investigated regional patterns of flood controlling processes and their temporal variability (Berghuijs et al., 2016; R Merz et al., 2020; Sikorska et al., 2015; Stein et al., 2020; Tarasova, Basso, & Merz, 2020; Tarasova, Basso, Wendi, et al., 2020; Tarouilly et al., 2021; W Yang et al., 2020). These studies categorize flood-generating rainfall using rainfall characteristics, for example, whether it is "short duration rain", "long duration rain", or "rainfall excess" (as compared to available soil moisture storage capacity). We take a somewhat different approach and classify flood-generating processes based on the physical processes that control precipitation or (in the case of snowmelt) moisture supply to the soil column. As noted above, precipitation caused by different meteorological processes responds to climate change differently, therefore, investigating historical changes of floods driven by different types of rainfall can help to understand the connection between large-scale hydroclimatic changes and changes in flooding, if and where they exist.

With this motivation, we develop a process-based flood classification method based on the meteorological processes that produce extreme precipitation and snowmelt events. We apply our classification scheme to the conterminous U.S. west of the Continental Divide (W-US) to categorize floods from 1960 to 2018 into one of six flood generating mechanisms (FGMs). We identify the dominant FGMs for 119 U.S. Geological Survey (USGS) stream gages and characterize changes in flood frequency, magnitude, and timing for each FGM. Our results provide new insights into how FGMs vary spatially and how floods of different FGMs have changed over the last six decades across the W-US.

2. Methods

2.1. Data

We used stream gages within the W-US from the USGS GAGES II reference database (Falcone, 2011). We removed stations with more than 20% missing data during 1960–2018 and with evidence of unreported upstream regulation such as reservoirs and diversions (Text S1 in the Supporting Information S1). This resulted in a total of 119 gages (Table S1 in the Supporting Information S1). We used daily mean streamflow (rather than

instantaneous peaks) due to data availability and length of records (Text S1 in the Supporting Information S1) similar to Archfield et al. (2016) and Berghuijs et al. (2016).

For each stream gauge, we used both the annual maximum series (AMS) and peaks over threshold (POT) for each water year (October-September) to represent flood events. For AMS we chose the floods with the largest daily discharge in each year. For POT, we set the threshold to ensure that two flood peaks per year were selected on average. We also select the upper-tail events (roughly the 10-year event) to focus on extreme floods (Text S1 in the Supporting Information S1). We then identified the FGMs for each AMS and POT event using observed and estimated hydroclimatic variables with a daily time step, including precipitation, surface air temperature, snow water equivalent (SWE), and snowmelt. We used the gridded precipitation and air temperature from observations produced by Livneh et al. (2015). The snow variables are output from the 1/16th degree spatial resolution Variable Infiltration Capacity (VIC) hydrology model run included in the Livneh et al. (2015) data set. The VIC model output was extensively evaluated and was shown to consistently reproduce observed SWE across the W-US (Ban et al., 2020; Li et al., 2019). We used the area-weighted mean of each hydroclimatic variable over the drainage area of the 119 basins to classify FGMs.

2.2. Assigning FGMs to Flood Events

We took the perspective that floods are primarily a response to intense moisture supply to the soil column (Slater & Villarini, 2016). We did not consider the effect of frozen soil, as it is not considered to be a "hydrologically important" factor across our domain (Storey, 1955). Similar to studies that categorize floods regionally (Sikorska et al., 2015; Tarasova, Basso, & Merz, 2020; Tarasova, Basso, Wendi, et al., 2020; W Yang et al., 2020), we first determined whether the moisture supply came from intense precipitation (referred to as rainfall hereafter) or snowmelt via a decision tree (Figure 1a). When substantial rain falls on a preexisting snowpack, snowmelt is induced by latent heating (augmented by longwave radiation) which directs moisture to the soil column, known as rain-on-snow (ROS) event (McCabe et al., 2007). We created a separate category for ROS floods which typically have a mixed moisture supply from rainfall and snowmelt (Figure 1a). For a flood event to be classified as ROS-related, we required that (a) the snowpack was isothermal at 0°C, (b) at least 25 mm day^{-1} of rainfall fell on a snowpack with at least 10 mm SWE, and (c) that ROS-related snowmelt made up at least 25% of the sum of the rainfall and snowmelt for the day (Li et al., 2019; Musselman et al., 2018; Text S2 in the Supporting Information S1). We classified other floods as snowmelt-driven (mostly by net radiation in spring or early summer) if snowmelt contributed more than 50% of the AMS flood daily discharge ($\text{mag}_{\text{snowmelt}} \geq 0.5$):

$$\text{mag}_{\text{snowmelt}} = \frac{\text{snowmelt}}{\text{snowmelt} + \text{rainfall}}$$

We used basin-averaged snowmelt and rainfall from Livneh-VIC model outputs, which have been shown to capture the signatures of SWE and streamflow (Li et al., 2019). We defined rainfall-driven floods as those that are not snowmelt driven ($\text{mag}_{\text{snowmelt}} < 0.5$).

We further partitioned rainfall-driven floods into convective (monsoons and non-monsoon convective) and large-scale frontal storms (AR and non-AR; Houze, 2014; Figure 1a). Convective storms mostly occur in the interior W-US and are produced by the mesoscale convective systems (MCS). We identified MCS events using the NOAA-CIRES CAPE data set (Compo et al., 2011), in conjunction with the gridded rainfall from Livneh-VIC. We chose 500 J kg^{-1} CAPE as the threshold for identifying MCS events (Holley et al., 2014; Kahraman et al., 2017). We partitioned convective storms occurring during the NAM season in the southwestern U.S. as monsoons. We defined the onset of the NAM for each station as the first three consecutive days of rainfall that exceeded 0.5 mm day^{-1} after July 1st (Higgins et al., 1999). We assumed that convective events occurring in the Southwest after the NAM onset through September 30th were monsoon related (L Yang et al., 2019). Frontal storms generally have longer durations, weaker atmospheric instability, and lower rainfall intensities than convective storms (Anagnostou, 2004). We classified non-convective rainfall-dominant floods as frontal storms (AR and non-AR related). We identified AR events using the intersection of AR events from Guan and Waliser (2015) and precipitation events on flood days, that is, floods that occur during AR days are labeled as AR driven. We classified the remaining frontal storms as non-AR.

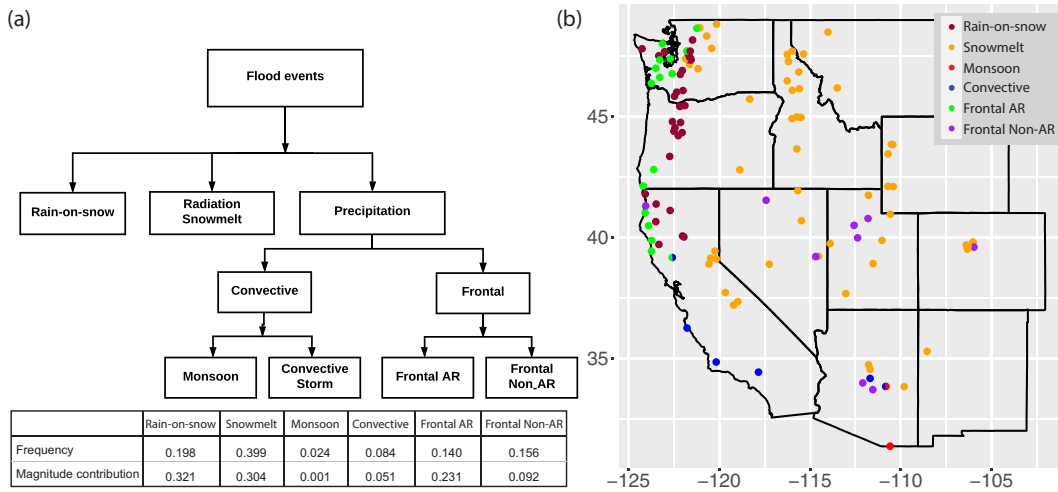

	Rain-on-snow	Snowmelt	Monsoon	Convective	Frontal AR	Frontal Non-AR
Frequency	0.198	0.399	0.024	0.084	0.140	0.156
Magnitude contribution	0.321	0.304	0.001	0.051	0.231	0.092

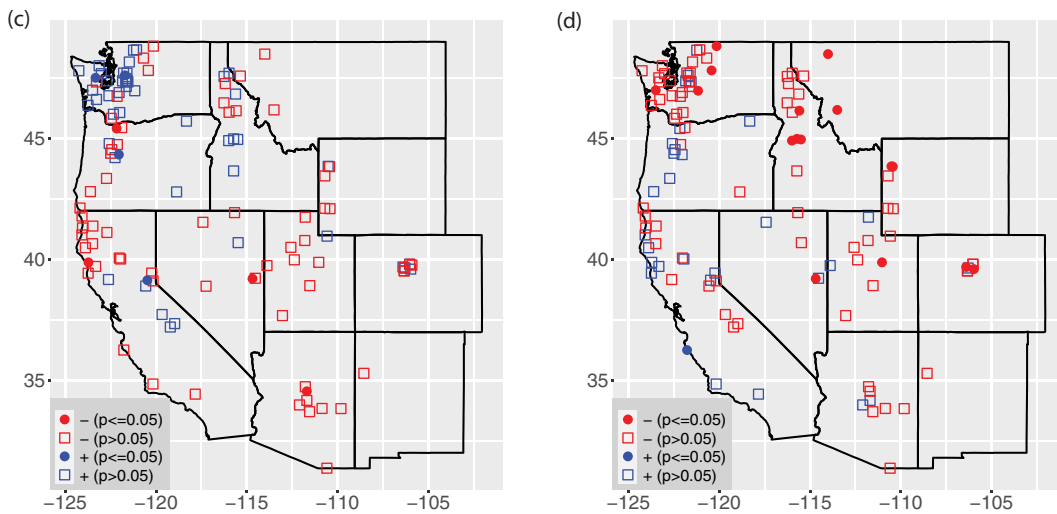

(e)

Dominant FGMs of basins	Flood Magnitude		Flood Timing	
	Increasing (p<0.05)	Decreasing (p<0.05)	Ealier (p<0.05)	Later (p<0.05)
Rain-on-snow	3	1	0	0
Snowmelt	1	1	13	0
Monsoon	0	0	0	0
Convective	0	0	0	1
Frontal AR	0	1	1	0
Frontal Non-AR	0	1	2	0
Total	4	4	16	1

Figure 1. (a) Decision tree to determine the flood generating mechanisms (FGMs) for each flood event at 119 basins. The table indicates the frequency and magnitude contribution of flood generating mechanisms (FGMs) among the annual maximum series (AMS) over all events during 1960–2018; (b) Dominant FGM for each basin based on the AMS during 1960–2018 (c–d) Trends of AMS magnitude (c) and timing (d) from 1960 to 2018. Filled dots indicate statistically significant trends with $p < 0.05$ while open squares indicate trends with $p > 0.05$. The red color in (c) indicates decreasing flood magnitude while the red color in (d) indicates change toward earlier floods; (e) The number of basins with statistically significant ($p < 0.05$) increasing trends and decreasing trends dominated by each FGM. The results for POT are qualitatively similar to AMS and are shown in Supporting Information (Table S2 and Figure S1 in the Supporting Information S1).

In summary, we analyzed daily streamflow from 1960 to 2018 across the W-US. For each gauge, we applied the decision tree (Figure 1a) to categorize each flood event into one of the six FGMs: ROS, radiation-driven snowmelt, monsoon convective storms (hereafter, monsoon), non-monsoon convective storms (hereafter convective

storms), frontal AR, and frontal non-AR. For each basin, we identified the dominant FGM as the FGM that occurred most frequently (largest fraction).

2.3. Frequency, Magnitude Contribution, and Timing of Each FGM

As we categorized each flood event into one of the six FGMs, we aggregated flood events caused by the same FGM and investigated the FGM's frequency, magnitude contribution, and timing across the W-US. We calculated the frequency of each FGM as the number of flood events associated with a specific FGM divided by the total number of flood events across the 119 basins over the 1960–2018 period. Similarly, we calculated the magnitude contribution as the daily maximum discharge for a specific FGM (at all sites) divided by the total runoff discharge at all sites for all FGMs during the same period. To investigate the changes in the FGMs' frequency and magnitude contribution with time, we calculated the frequency (magnitude contribution) of each FGM in a year and estimated the trends from 1960 to 2018. We further examined ROS frequency as a function of basin elevation (see Figure S5 in the Supporting Information S1).

For each FGM, we calculated the mean flood dates averaged over all events associated with that FGM in a year and estimated the trends of mean flood date for that FGM from 1960 to 2018. Since flood timing has large inter-station differences, we use a representative flood date for each flood event, which is defined as the flood date for each event in the given FGM minus the mean flood date for that FGM and station.

2.4. Trend Analysis

We used the Theil-Sen slope estimator (Sen, 1968; Theil, 1992) to estimate trends in AMS and POT magnitude and timing for each station as well as the trends in flood frequency, magnitude, and timing for each FGM across all stations. We used the modified Mann-Kendall test (Hamed & Rao, 1998; Mann, 1945) to determine the trends' statistical significance. Additionally, we evaluated the overall significance across the entire W-US and hydrologic region level, referred to as field significance (Livezey & Chen, 1983) of trends across all stations. Local significance (via the Mann-Kendall test) determines whether each local null hypothesis is true at a given significance level; while field significance essentially determines whether multiple rejections of the null hypothesis at the local level (in our case, the significant flood trends at multiple stations) might be a manifestation of spatially correlated noise. The field significance tests were conducted following Douglas et al. (2000) to account for the spatial cross-correlation of streamflow (Text S3 in the Supporting Information S1).

3. Results

3.1. Flood Generating Mechanisms (FGMs)

The table within Figure 1a shows the frequency and magnitude contribution of each FGM (i.e., the fractions of all AMS events and total flood discharge, respectively). Of all events across the 119 USGS gages from 1960 to 2018, radiation-driven snowmelt is the most frequently occurring FGM (39.9%) and the second-largest contributor to the AMS magnitude (30.4%). ROS floods account for about 19.8% by frequency and 32.1% by magnitude of all floods. Frontal AR and non-AR account for 14% and 15.6% by frequency and 23.1% and 9.2% by magnitude, respectively. Monsoon and convective storms combined contribute 10.8% by frequency and an even smaller percentage (5.2%) by magnitude of all events. The FGM contributions using POT are similar to the AMS contributions (see Supporting Information S1). In comparison to AMS, frequency and magnitude contributions of snowmelt, frontal AR, and convective-related floods are slightly larger than for POT with differences less than 2%; while ROS, frontal non-AR, and monsoon-driven floods are slightly smaller for POT (Table S1 in the Supporting Information S1). For upper-tail events, ROS becomes the most important FGM as compared to all AMS events, contributing as much as snowmelt for frequency (33% for both ROS and snowmelt) and more than any other FGM for flood magnitude (44% for ROS).

The dominant FGMs show strong regional patterns, with frontal storms prevalent in basins along the coastal portion of our domain and radiation-driven snowmelt events dominating the interior (Figure 1b). AR-dominant floods occur along the coastal portion of the Pacific Northwest (Figure 1b, shown in more detail in Figure S2 in the Supporting Information S1) and are often associated with Pacific storm tracks (Ralph & Dettinger, 2011; Stohl et al., 2008). ROS is the dominant FGM for basins in coastal maritime climates, for example, basins along

the western side of the Cascade Mountains. We note that our ROS category in many cases is associated with winter storms that otherwise would be classified as frontal AR and non-AR. Floods driven by AR storms dominate in the Pacific Northwest and Klamath Mountains (Northern California) and floods driven by frontal non-AR dominate parts of the Great Basin and Southwest. For stations in the Pacific Northwest and Northern California, the dominant FGM accounts for 30%–40% of total events (Figure S3a in the Supporting Information S1) with floods in those areas caused by a mixture of frontal AR, frontal non-AR, and ROS. Radiation-driven snowmelt events account for more than 60% of AMS for most basins in the interior (Figure S3a in the Supporting Information S1). This is the primary FGM in basins east of the Cascade Mountains east to Wyoming, in the Sierra Nevada, and sporadically throughout mountain ranges of the Southwest (Figure 1b). Convective storms are the dominant FGM in Southern California and Arizona where many stations have secondary FGMs, (e.g., monsoons; see Figure S2 in the Supporting Information S1). Monsoon-driven floods are concentrated in Southern Arizona (Figure S2c in the Supporting Information S1), where floods mostly occur during the NAM season in late summer. The spatial distribution of dominant FGMs for POT floods are highly consistent with that for AMS floods (Figure S1 in the Supporting Information S1).

Our classification corroborates results from previous studies, which show that ARs dominate flood events in the Pacific Northwest and coastal northern California, and that ROS is the dominant FGM throughout the Washington and Oregon Cascades (Barth et al., 2017; Konrad & Dettinger, 2017; Marks et al., 1998; McCabe et al., 2007; Ralph et al., 2006, 2011). For 70% of basins across our study domain, the dominant FGM accounts for more than 50% of all flood events (Figure S3b in the Supporting Information S1). We note that certain regions, such as the Southwest, have relatively sparse gage distributions. Our study nonetheless shows that FGMs have fairly well-defined domains relative to their moisture supply. These results should be (at least in a general sense) applicable to regions within the domain where the station density is modest. We next examine how flood risk associated with the FGMs has varied in space and time during our study period.

3.2. Trends in Flood Magnitude and Timing

We find that only eight of the 119 stations (6.7%) have statistically significant trends ($p < 0.05$; Figure 1e) in flood magnitude. Of these, four stations within the Pacific Northwest have statistically significantly increasing trends, and four stations (located in Arizona, California, Nevada, and Oregon) have statistically significantly decreasing trends. In contrast, the corresponding basin-averaged precipitation from Livneh shows statistically significant uptrends in seven stations (mostly in Washington) and significant downtrends in five stations (in Northern California and Oregon; Figure S4a in the Supporting Information S1). Despite statistically significant precipitation increases in Washington, the corresponding changes in flooding in that area were not statistically significant. One possible explanation may be antecedent soil moisture which can modulate the effects of increasing rainfall (Ivancic & Shaw, 2015). Temperature increases which drive increases in rainfall also decrease soil moisture. This increases the required incident rainfall for flooding, so that storms that occurred in the early record that might have produced flooding might not have produced floods in the later record (even with increased precipitation intensities; Cao et al., 2020). Throughout the W-US basins or at hydrologic region level, changes in AMS magnitude have weak geographic cohesion and the trends are not field significant ($p = 0.05$).

We also investigate changes in the timing of AMS for each basin, which show an overall earlier shift across the W-US (Figure 1d), especially in radiation-snowmelt dominant basins. 16 out of 119 (13.4%) basins show significant shifts toward earlier dates, while one basin has a significant shift toward later dates (Figure 1e). The trends in AMS timing are not field-significant (at $p = 0.05$) across the W-US or at hydrologic region level. Among the 16 basins with an earlier shift, 13 are dominated by radiation-driven snowmelt. The flood timing changes in these basins are associated with an earlier onset of springtime snowmelt due to increasing temperatures (Figure S4b in the Supporting Information S1). Generally, we find that only a few stations exhibit significant trends in AMS magnitude and timing despite widespread and significant changes in atmospheric forcing -- for example, rainfall increases (in the Pacific Northwest), and generally warming air temperature throughout W-US. An analysis of POT floods (Figure S1b in the Supporting Information S1) leads to a similar conclusion as AMS.

Our basin-scale analyses indicate at most tenuous links between climate change and flooding (aside from the snowmelt FGM) suggesting that other factors may play a role, such as rainfall phase and duration, antecedent soil moisture, and catchment geometry (Wasko & Sharma, 2015). Further research will be necessary to quantify

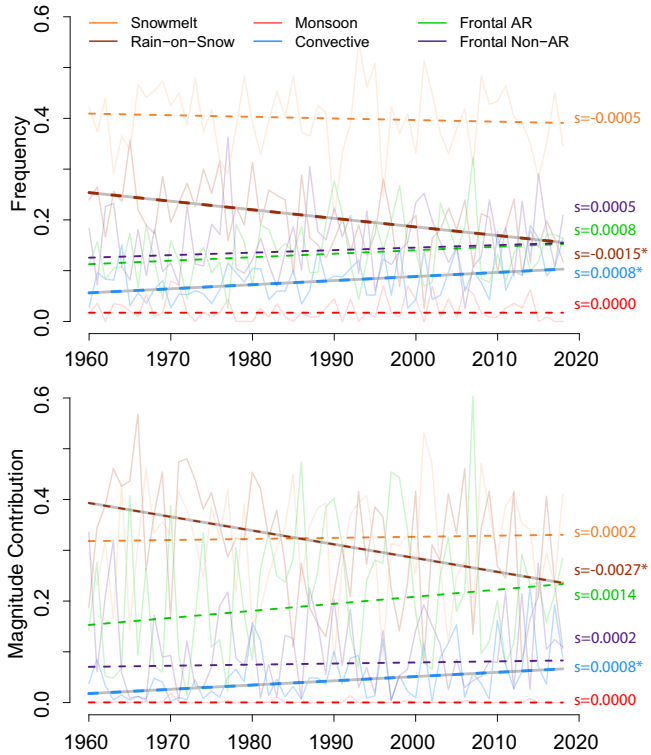

Figure 2. Trends in the (a) frequency and (b) magnitude contribution of six flood generating mechanisms (FGMs) for the W-US basins over the period 1960–2018 calculated by Theil-Sen slope (yr^{-1}). Asterisk indicates that trends are significant at the 0.05 level in the Mann-Kendall test and "s" represents the slope of the Theil-Sen test. For each year, the frequency of an FGM is calculated using flood counts associated with the FGM divided by the total flood counts; the magnitude contribution of an FGM is calculated using the daily maximum discharge for all events associated with the FGM divided by the total daily maximum discharge among all basins.

the influence of catchment conditions on the climate change-extreme runoff relationship at the regional, continental, and global scales.

3.3. Trends in Flood Frequency, Magnitude, and Timing by FGM

We investigated changes in the frequency, magnitude, and timing of floods for each FGM across the W-US. Among the six FGMs, only two had significant changes ($p < 0.05$) over our study period (Figure 2a). The frequency of ROS-induced floods significantly decreased by 0.0015 $years^{-1}$ ($p < 0.01$) during 1960–2018, which is equivalent to a reduction of about 10 events during our study period across the W-US. The decrease in ROS-induced flood frequency is comes mostly from low-to-mid elevation basins (lower than 1,500 m), whereas there are no statistically significant trends in ROS floods for the highest elevation basins (Figure S5 in the Supporting Information S1). The magnitude contribution of ROS-induced floods has experienced an even larger decrease by 0.0027 $years^{-1}$ with $p < 0.05$ (Figure 2b). These decreases are likely related to reduced snowpack, which is sensitive to increasing temperatures across the mountainous W-US (McCabe et al., 2007; Musselman et al., 2018). Decreasing ROS-driven flood frequency and magnitude have also been found in Western Europe at lower elevations (Fischer & Schumann, 2020; Fischer et al., 2019; Freudiger et al., 2014). Interestingly, these results contrast with those found by Dethier et al. (2020), who observed statistically significant increases in annual flood frequency as well as early snowpack depletion. Furthermore, snowmelt-driven floods have been found to be transforming to ROS-driven floods in Eastern Europe, leading to increases in ROS flood frequency there (Kemter et al., 2020).

Convective-storm related floods have a statistically significant positive trend ($p < 0.05$) in both frequency and magnitude contribution (Figure 2), although they account for only about 8% of flood frequency and 5% of flood discharge, respectively (Figure 1a). The increase in convective storm-related floods may be related to increases in CAPE throughout the Southwest, which makes the environment more favorable for convection and allows MCSs to become larger (Feng et al., 2016; Prein et al., 2017). Changes in convective-driven floods have not been widely studied globally. Still, our results corroborate with Llasat et al. (2016, 2021) who showed the positive trends in flash floods in Mediterranean Spain partially related to increasing convective precipitations. Aside from increases in convective-storm related floods, we also find a slight increase in AR-driven flood frequency, which however is only weakly significant ($p = 0.08$) in comparison to ROS and convective storm floods. We do not identify statistically significant long-term trends in frequency or intensity of other FGMs.

FGM trends are similar for POT events (Table S3 in the Supporting Information S1), where we find significantly decreasing trends ($p < 0.05$) in ROS flood frequency (-0.0008 $years^{-1}$) and magnitude contribution (-0.0022 $years^{-1}$). Convective storm floods showed a significant increasing trend ($p < 0.05$) in magnitude contribution, but the positive trend in frequency is less significant in POT events ($p = 0.07$) than in AMS. We find a statistically significant increase ($p = 0.04$) in the frequency of AR-related floods in the POT series, which is more significant than the AMS series in Figure 2b. For the upper tail events, we do not observe statistically significant changes in frequency or magnitude contribution of any FGM, which may be due to the small number of events included (typically 10 events per year across W-US).

Trends in flood timing by FGM are shown in Figure 3. Floods dominated by radiation snowmelt have a significant negative trend in flood timing of -0.16 days yr^{-1}, equivalent to an earlier shift on average by about nine days from 1960 to 2018. The earlier trends in snowmelt floods are caused by diminishing winter snow accumulations and warmer temperatures during the melting season (Figure S4b in the Supporting Information S1), as observed in the W-US (Dudley et al., 2017; Stewart et al., 2005) and northeastern Europe (Bloschl et al., 2017). For the remaining FGMs, we do not identify any statistically significant trends in flood timing.

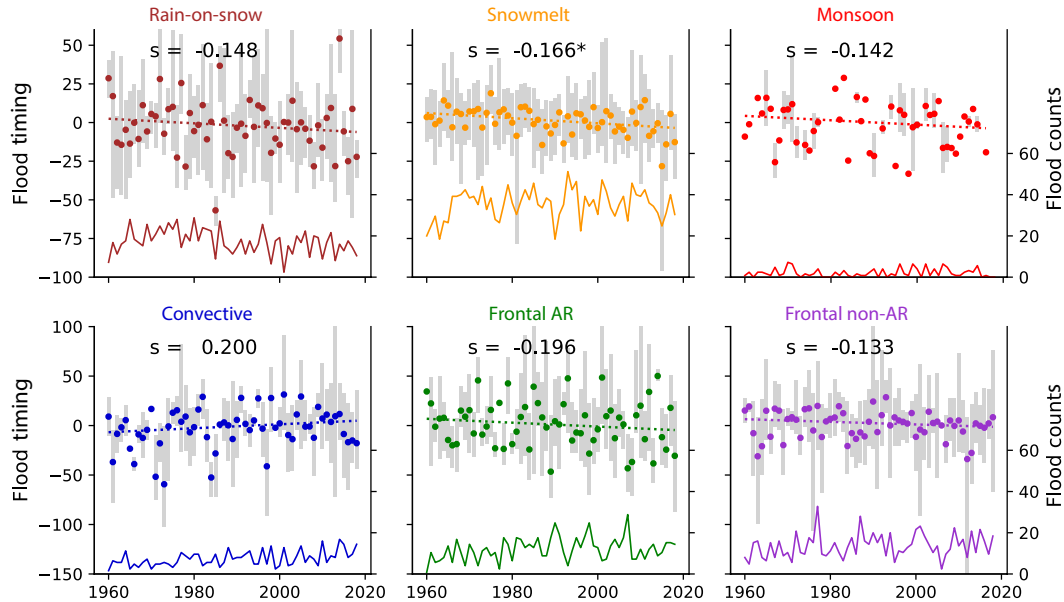

Figure 3. Trend magnitudes (day yr^{-1}) of mean flood timing for each flood generating mechanisms (FGM) across W-US. For each FGM, the Gy bar indicates 0.1 and 0.9 quantiles of flood timing, and the color-coded dots indicate the mean flood timing averaged over all events associated with that FGM in each year. The color-coded lines indicate flood counts caused by each FGM in a year. Trends were calculated using the Theil-Sen slope and "s" represents the trend magnitude of Theil-Sen slope. The asterisk indicates that the trend is significant at the 0.05 level in the Mann-Kendall test.

4. Conclusions

Throughout the W-US, radiation-driven snowmelt is the dominant contributor to flood frequency, while frontal non-AR rainfall is the greatest contributor to flood magnitudes. Floods throughout the coastal W-US are dominated by AR events, a substantial portion of which are ROS-related. Floods in the central and northern interior of W-US are mostly associated with radiation-driven snowmelt. Monsoon and convective storms contribute a much smaller fraction of floods in the W-US interior. Although pronounced temperature increases have changed the intensity, as well as the spatial and temporal variability of precipitation extremes across the region, changes in flood frequency, magnitude, and timing are more complex:

1. ROS-related flood frequency and magnitudes have decreased significantly across the W-US
2. The timing of floods caused by radiation snowmelt has shifted earlier, consistent with earlier snowmelt onset corresponding to widespread warming in the mountainous W-US
3. There has been a statistically significant increase in convective storm-related flood frequency and magnitudes, mostly associated with floods occurring in the Southwest
4. Aside from above changes, the magnitude, frequency, and timing of floods across the western U.S. not associated with snow processes have been relatively stable over the last 60 years

The trends we observe in the frequency of ROS and the timing of radiation snowmelt-driven floods are likely to continue in a warming climate as they are strongly temperature-related. Likewise, the changes in frequency and magnitude of convective storm-related floods may well be temperature-related in which case they are likely to continue to increase in the future. While convective storm-related floods account for a small portion of the total flood counts and flood discharge across W-US, they could have important implications in the Southwest, especially for flash floods.

It is worth noting that the spatial scale of convective storms generally is smaller than that of winter storms, or the SWE and net radiation anomalies that drive spring snowmelt floods. Accordingly, the linkage between flood forcing (intense rainfall) and response tends to be more direct with convective storms, when compared with other FGMs. In this respect, changes in convective storm-associated flooding we observe may represent the tip of the iceberg, so to speak. Further study is needed as the USGS stream gage network used in this study does not include

many sites with drainage areas that are comparable to the spatial scales of convective storms, and hence results may well under-represent this FGM. The prognosis for future alterations to the magnitude of changes for FGM categories other than convective and snow-related (ROS and radiation snowmelt) is less clear, as they result from complicated interactions of rainfall extremes (which are likely to increase), antecedent soil moisture (likely to decrease), storm timing (direction of changes not clear) as well as other factors such as storm extent.

Data Availability Statement

NOAA-CIRES CAPE data set are from the NOAA/OAR/ESRL PSL Web site at https://psl.noaa.gov/data/gridded/data.20thC_ReanV2c.monolevel.html; The daily streamflow from USGS GAGES II reference database is available at https://water.usgs.gov/GIS/metadata/usgswrd/XML/gagesII_Sept2011.xml. We uploaded the data used in this paper on https://doi.org/10.5281/zenodo.5678009.

Acknowledgments
We thank Matthew Cooper of the Pacific Northwest National Laboratory and Kayden Haleakala of the Department of Civil & Environmental Engineering, UCLA for making available their pre-processed versions of the USGS GAGES-II data. We thank Lu Su of Department of Geography, UCLA for extending the Livneh-VIC data to the most recent years. We would also like to thank Matthew Zebrowski, Department of Geography, UCLA, for assisting with illustrating the figures. Portions of this material are based upon work supported by the National Science Foundation Graduate Research Fellowship Program under Grant No. DGE-2034835.

References

Anagnostou, E. N. (2004). A convective/stratiform precipitation classification algorithm for volume scanning weather radar observations. *Meteorological Applications*, *11*(4), 291–300. https://doi.org/10.1017/s1350482704001409

Archfield, S. A., Hirsch, R. M., Viglione, A., & Bloschl, G. (2016). Fragmented patterns of flood change across the United States. *Geophysical Research Letters*, *43*, 10232–10239. https://doi.org/10.1002/2016gl070590

Ban, Z., Das, T., Cayan, D., Xiao, M., & Lettenmaier, D. P. (2020). Understanding the asymmetry of annual streamflow responses to seasonal warming in the Western United States. *Water Resources Research*, *56*(12), e2020WR027158. https://doi.org/10.1029/2020wr027158

Barth, N. A., Villarini, G., Nayak, M. A., & White, K. (2017). Mixed populations and annual flood frequency estimates in the western United States: The role of atmospheric rivers. *Water Resources Research*, *53*(1), 257–269. https://doi.org/10.1002/2016wr019064

Barth, N. A., Villarini, G., & White, K. (2018). Contribution of eastern North Pacific tropical cyclones and their remnants on flooding in the western United States. *International Journal of Climatology*, *38*(14), 5441–5446. https://doi.org/10.1002/joc.5735

Barth, N. A., Villarini, G., & White, K. (2019). Accounting for mixed populations in flood frequency analysis: Bulletin 17C perspective. *Journal of Hydrologic Engineering*, *24*(3), 04019002. https://doi.org/10.1061/(asce)he.1943-5584.0001762.

Berg, P., Moseley, C., & Haerter, J. O. (2013). Strong increase in convective precipitation in response to higher temperatures. *Nature Geoscience*, *6*(3), 181–185. https://doi.org/10.1038/ngeo1731

Berghuijs, W. R., Woods, R. A., & Hrachowitz, M. (2014). A precipitation shift from snow towards rain leads to a decrease in streamflow. *Nature Climate Change*, *4*(7), 583–586. https://doi.org/10.1038/nclimate2246

Berghuijs, W. R., Woods, R. A., Hutton, C. J., & Sivapalan, M. (2016). Dominant flood generating mechanisms across the United States. *Geophysical Research Letters*, *43*, 4382–4390. https://doi.org/10.1002/2016gl068070

Bindoff, N. L., Stott, P. A., AchutaRao, K. M., Allen, M. R., Gillett, N., Gutzler, D., et al. (2013). Detection and attribution of climate change: From global to regional. In T. F. Stocker, D. Qin, G.-K. Plattner, M. Tignor, S. K. Allen, J. Boschung, et al. (Eds.), *Climate change 2013: The physical science basis. Contribution of working group I to the fifth assessment report of the intergovernmental panel on climate change* (pp. 867–952). Cambridge University Press.

Bloschl, G., Hall, J., Parajka, J., Perdigão, R. A., Merz, B., Arheimer, B., et al. (2017). Changing climate shifts timing of European floods. *Science*, *357*(6351), 588–590.

Bloschl, G., Nester, T., Komma, J., Parajka, J., & Perdigao, R. A. P. (2013). The June 2013 flood in the upper danube basin, and comparisons with the 2002, 1954 and 1899 floods. *Hydrology and Earth System Sciences*, *17*(12), 5197–5212. https://doi.org/10.5194/hess-17-5197-2013

Blum, A. G., Ferraro, P. J., Archfield, S. A., & Ryberg, K. R. (2020). Causal effect of impervious cover on annual flood magnitude for the United States. *Geophysical Research Letters*, *47*, e2019GL086480. https://doi.org/10.1029/2019gl086480

Cao, Q., Gershunov, A., Shulgina, T., Ralph, F. M., Sun, N., & Lettenmaier, D. P. (2020). Floods due to atmospheric rivers along the US West coast: The role of antecedent soil moisture in a Warming climate. *Journal of Hydrometeorology*, *21*(8), 1827–1845. https://doi.org/10.1175/jhm-d-19-0242.1

Compo, G. P., Whitaker, J. S., Sardeshmukh, P. D., Matsui, N., Allan, R. J., Yin, X., et al. (2011). The twentieth century reanalysis project. *The Quarterly Journal of the Royal Meteorological Society*, *137*(654), 1–28. https://doi.org/10.1002/qj.776

Davenport, F. V., Herrera-Estrada, J. E., Burke, M., & Diffenbaugh, N. S. (2020). Flood size increases nonlinearly across the western United States in response to lower snow-precipitation ratios. *Water Resources Research*, *56*(1), e2019WR025571. https://doi.org/10.1029/2019wr025571

Dethier, E. N., Sartain, S. L., Renshaw, C. E., & Magilligan, F. J. (2020). Spatially coherent regional changes in seasonal extreme streamflow events in the United States and Canada since 1950. *Science Advances*, *6*(49), eaba5939. https://doi.org/10.1126/sciadv.aba5939

Dettinger, M. D., & Cayan, D. R. (1995). Large-scale atmospheric forcing of recent trends toward early snowmelt runoff in California. *Journal of Climate*, *8*(3), 606–623. https://doi.org/10.1175/1520-0442(1995)008<0606:lsafor>2.0.co;2

Do, H. X., Westra, S., & Leonard, M. (2017). A global-scale investigation of trends in annual maximum streamflow. *Journal of Hydrology*, *552*, 28–43. https://doi.org/10.1016/j.jhydrol.2017.06.015

Donat, M. G., Alexander, L. V., Yang, H., Durre, I., Vose, R., Dunn, R. J., et al. (2013). Updated analyses of temperature and precipitation extreme indices since the beginning of the twentieth century: The HadEX2 dataset. *Journal of Geophysical Research: Atmospheres*, *118*, 2098–2118. https://doi.org/10.1002/jgrd.50150

Douglas, E. M., Vogel, R. M., & Kroll, C. N. (2000). Trends in floods and low flows in the United States: Impact of spatial correlation. *Journal of Hydrology*, *240*(1–2), 90–105. https://doi.org/10.1016/s0022-1694(00)00336-x

Downton, M. W., Miller, J. Z. B., & Pielke, R. A. (2005). Reanalysis of U.S. National Weather service flood loss database. *Natural Hazards Review*, *6*(1), 13–22. https://doi.org/10.1061/(asce)1527-6988(2005)6:1(13).

Dudley, R. W., Hodgkins, G. A., McHale, M. R., Kolian, M. J., & Renard, B. (2017). Trends in snowmelt-related streamflow timing in the conterminous United States. *Journal of Hydrology*, *547*, 208–221. https://doi.org/10.1016/j.jhydrol.2017.01.051

Falcone, J. A. (2011). *GAGES-II: Geospatial attributes of gages for evaluating streamflow*. US Geological Survey. https://doi.org/10.3133/70046617

Fayne, J. V., Ahamed, A., Roberts-Pierel, J., Rumsey, A. C., & Kirschbaum, D. (2019). Automated satellite-cased landslide identification product for Nepal. *Earth Interactions*, *23*(3), 1–21. https://doi.org/10.1175/ei-d-17-0022.1

Feng, Z., Leung, L. R., Hagos, S., Houze, R. A., Burleyson, C. D., & Balaguru, K. (2016). More frequent intense and long-lived storms dominate the springtime trend in central US rainfall. *Nature Communications*, *7*. https://doi.org/10.1038/ncomms13429

Fischer, S., & Schumann, A. (2020). Spatio-temporal consideration of the impact of flood event types on flood statistic. *Stochastic Environmental Research and Risk Assessment*, *34*(9), 1331–1351. https://doi.org/10.1007/s00477-019-01690-2

Fischer, S., Schumann, A., & Buhler, P. (2019). Timescale-based flood typing to estimate temporal changes in flood frequencies. *Hydrological Sciences Journal*, *64*(15), 1867–1892. https://doi.org/10.1080/02626667.2019.1679376

Freudiger, D., Kohn, I., Stahl, K., & Weiler, M. (2014). Large-scale analysis of changing frequencies of rain-on-snow events with flood-generation potential. *Hydrology and Earth System Sciences*, *18*(7), 2695–2709. https://doi.org/10.5194/hess-18-2695-2014

Gershunov, A., Shulgina, T., Ralph, F. M., Lavers, D. A., & Rutz, J. J. (2017). Assessing the climate-scale variability of atmospheric rivers affecting western North America. *Geophysical Research Letters*, *44*, 7900–7908. https://doi.org/10.1002/2017gl074175

Guan, B., & Waliser, D. E. (2015). Detection of atmospheric rivers: Evaluation and application of an algorithm for global studies. *Journal of Geophysical Research: Atmospheres*, *120*, 12514–12535. https://doi.org/10.1002/2015jd024257

Hall, J., Arheimer, B., Borga, M., Brázdil, R., Claps, P., Kiss, A., et al. (2014). Understanding flood regime changes in Europe: A state-of-the-art assessment. *Hydrology and Earth System Sciences*, *18*(7), 2735–2772. https://doi.org/10.5194/hess-18-2735-2014

Hamed, K. H., & Rao, A. R. (1998). A modified Mann-Kendall trend test for autocorrelated data. *Journal of Hydrology*, *204*(1–4), 182–196. https://doi.org/10.1016/s0022-1694(97)00125-x

Higgins, R. W., Chen, Y., & Douglas, A. V. (1999). Interannual variability of the North American warm season precipitation regime. *Journal of Climate*, *12*(3), 653–680. https://doi.org/10.1175/1520-0442(1999)012<0653:ivotna>2.0.co;2

Hodgkins, G. A., Whitfield, P. H., Burn, D. H., Hannaford, J., Renard, B., Stahl, K., et al. (2017). Climate-driven variability in the occurrence of major floods across North America and Europe. *Journal of Hydrology*, *552*, 704–717. https://doi.org/10.1016/j.jhydrol.2017.07.027

Holley, D. M., Dorling, S. R., Steele, C. J., & Earl, N. (2014). A climatology of convective available potential energy in Great Britain. *International Journal of Climatology*, *34*(14), 3811–3824. https://doi.org/10.1002/joc.3976

Houze, R. A. (2014). Types of Clouds in Earth's Atmosphere. *Cloud Dynamics* (Vol. 104, 2nd ed., pp. 3–23). https://doi.org/10.1016/B978-0-12-374266-7.00001-9

Huang, H., Xue, Y., Chilukoti, N., Liu, Y., Chen, G., & Diallo, I. (2020). Assessing global and regional effects of reconstructed land-use and land-cover change on climate since 1950 using a coupled land–atmosphere–ocean model. *Journal of Climate*, *33*(20), 8997–9013. https://doi.org/10.1175/jcli-d-20-0108.1

Huang, X., Swain, D. L., & Hall, A. D. (2020). Future precipitation increase from very high resolution ensemble downscaling of extreme atmospheric river storms in California. *Science Advances*, *6*(29), eaba1323. https://doi.org/10.1126/sciadv.aba1323

Ivancic, T. J., & Shaw, S. B. (2015). Examining why trends in very heavy precipitation should not be mistaken for trends in very high river discharge. *Climatic Change*, *133*(4), 681–693. https://doi.org/10.1007/s10584-015-1476-1

Kahraman, A., Kadioglu, M., & Markowski, P. M. (2017). Severe convective storm environments in Turkey. *Monthly Weather Review*, *145*(12), 4711–4725. https://doi.org/10.1175/mwr-d-16-0338.1

Kemter, M., Merz, B., Marwan, N., Vorogushyn, S., & Bloschl, G. (2020). Joint trends in flood magnitudes and spatial extents across Europe. *Geophysical Research Letters*, *47*, e2020GL087464. https://doi.org/10.1029/2020gl087464

Kendon, E. J., Roberts, N. M., Fowler, H. J., Roberts, M. J., Chan, S. C., & Senior, C. A. (2014). Heavier summer downpours with climate change revealed by weather forecast resolution model. *Nature Climate Change*, *4*(7), 570–576. https://doi.org/10.1038/nclimate2258

Konrad, C. P., & Dettinger, M. D. (2017). Flood runoff in relation to Water vapor transport by atmospheric rivers over the Western United States, 1949-2015. *Geophysical Research Letters*, *44*, 11456–11462. https://doi.org/10.1002/2017gl075399

Lenderink, G., & Van Meijgaard, E. (2008). Increase in hourly precipitation extremes beyond expectations from temperature changes. *Nature Geoscience*, *1*(8), 511–514. https://doi.org/10.1038/ngeo262

Li, D., Lettenmaier, D. P., Margulis, S. A., & Andreadis, K. (2019). The role of rain-on-snow in flooding over the conterminous United States. *Water Resources Research*, *55*(11), 8492–8513. https://doi.org/10.1029/2019wr024950

Lins, H. F., & Slack, J. R. (1999). Streamflow trends in the United States. *Geophysical Research Letters*, *26*(2), 227–230. https://doi.org/10.1029/1998gl900291

Livezey, R. E., & Chen, W. Y. (1983). Statistical field significance and its determination by Monte-carlo techniques. *Monthly Weather Review*, *111*(1), 46–59. https://doi.org/10.1175/1520-0493(1983)111<0046:sfsaid>2.0.co;2

Livneh, B., Bohn, T. J., Pierce, D. W., Munoz-Arriola, F., Nijssen, B., Vose, R., et al. (2015). A spatially comprehensive, hydrometeorological data set for Mexico, the U.S., and Southern Canada 1950–2013. *Scientific Data*, *2*, 150042. https://doi.org/10.1038/sdata.2015.42

Llasat, M. C., del Moral, A., Cortes, M., & Rigo, T. (2021). Convective precipitation trends in the Spanish Mediterranean region. *Atmospheric Research*, *257*, 105581. https://doi.org/10.1016/j.atmosres.2021.105581

Llasat, M. C., Marcos, R., Turco, M., Gilabert, J., & Llasat-Botija, M. (2016). Trends in flash flood events versus convective precipitation in the Mediterranean region: The case of Catalonia. *Journal of Hydrology*, *541*, 24–37. https://doi.org/10.1016/j.jhydrol.2016.05.040

Mann, H. B. (1945). Nonparametric tests against trend. *Econometrica*, *13*(3), 245–259. https://doi.org/10.2307/1907187

Marks, D., Kimball, J., Tingey, D., & Link, T. (1998). The sensitivity of snowmelt processes to climate conditions and forest cover during rain-on-snow: A case study of the 1996 Pacific Northwest flood. *Hydrological Processes*, *12*(10-11), 1569–1587. https://doi.org/10.1002/(sici)1099-1085(199808/09)12:10/11<1569::aid-hyp682>3.0.co;2-l

Mass, C., Skalenakis, A., & Warner, M. (2011). Extreme precipitation over the West coast of north America: Is there a trend? *Journal of Hydrometeorology*, *12*(2), 310–318. https://doi.org/10.1175/2010jhm1341.1

McCabe, G. J., Clark, M. P., & Hay, L. E. (2007). Rain-on-snow events in the western United States. *Bulletin of the American Meteorological Society*, *88*(3), 319–328. https://doi.org/10.1175/bams-88-3-319

Merz, B., Vorogushyn, S., Uhlemann, S., Delgado, J., & Hundecha, Y. (2012). HESS Opinions 'More efforts and scientific rigour are needed to attribute trends in flood time series. *Hydrology and Earth System Sciences*, *16*(5), 1379–1387. https://doi.org/10.5194/hess-16-1379-2012

Merz, R., Tarasova, L., & Basso, S. (2020). The flood cooking book: Ingredients and regional flavors of floods across Germany. *Environmental Research Letters*, *15*(11), 114024. https://doi.org/10.1088/1748-9326/abb9dd

Min, S. K., Zhang, X. B., Zwiers, F. W., & Hegerl, G. C. (2011). Human contribution to more-intense precipitation extremes. *Nature*, *470*(7334), 378–381. https://doi.org/10.1038/nature09763

Musselman, K. N., Lehner, F., Ikeda, K., Clark, M. P., Prein, A. F., Liu, C. H., et al. (2018). Projected increases and shifts in rain-on-snow flood risk over western North America. *Nature Climate Change*, *8*(9), 808–812. https://doi.org/10.1038/s41558-018-0236-4

Pall, P., Aina, T., Stone, D. A., Stott, P. A., Nozawa, T., Hilberts, A. G. J., et al. (2011). Anthropogenic greenhouse gas contribution to flood risk in England and Wales in autumn 2000. *Nature*, *470*(7334), 382–385. https://doi.org/10.1038/nature09762

Perez, G., Gomez-Velez, J. D., Mantilla, R., Wright, D. B., & Li, Z. (2021). The effect of storm direction on flood frequency analysis. *Geophysical Research Letters*, *48*, e2020GL091918. https://doi.org/10.1029/2020gl091918

Prein, A. F., Liu, C. H., Ikeda, K., Trier, S. B., Rasmussen, R. M., Holland, G. J., & Clark, M. P. (2017). Increased rainfall volume from future convective storms in the US. *Nature Climate Change*, *7*(12), 880–840. https://doi.org/10.1038/s41558-017-0007-7

Ralph, F. M., & Dettinger, M. D. (2011). Storms, floods, and the science of atmospheric rivers. *Eos, Transactions American Geophysical Union*, *92*(32), 265–266. https://doi.org/10.1029/2011eo320001

Ralph, F. M., Dettinger, M. D., Rutz, J., & Waliser, E. (2020). *Atmospheric rivers*. Springer Nature. https://doi.org/10.1007/978-3-030-28906-5

Ralph, F. M., Neiman, P. J., Kiladis, G. N., Weickmann, K., & Reynolds, D. W. (2011). A Multiscale observational case study of a pacific atmospheric river exhibiting tropical-extratropical connections and a mesoscale frontal wave. *Monthly Weather Review*, *139*(4), 1169–1189. https://doi.org/10.1175/2010mwr3596.1

Ralph, F. M., Neiman, P. J., Wick, G. A., Gutman, S. I., Dettinger, M. D., Cayan, D. R., & White, A. B. (2006). Flooding on California's Russian River: Role of atmospheric rivers. *Geophysical Research Letters*, *33*, L13801. https://doi.org/10.1029/2006gl026689

Sen, P. K. (1968). Estimates of the regression coefficient based on Kendall's tau. *Journal of the American Statistical Association*, *63*(324), 1379–1389. https://doi.org/10.1080/01621459.1968.10480934

Sharma, A., Wasko, C., & Lettenmaier, D. P. (2018). If precipitation extremes are increasing, Why aren't floods? *Water Resources Research*, *54*(11), 8545–8551. https://doi.org/10.1029/2018wr023749

Sikorska, A. E., Viviroli, D., & Seibert, J. (2015). Flood-type classification in mountainous catchments using crisp and fuzzy decision trees. *Water Resources Research*, *51*(10), 7959–7976. https://doi.org/10.1002/2015wr017326

Slater, L. J., & Villarini, G. (2016). Recent trends in US flood risk. *Geophysical Research Letters*, *43*, 12428–12436. https://doi.org/10.1002/2016gl071199

Stein, L., Pianosi, F., & Woods, R. (2020). Event-based classification for global study of river flood generating processes. *Hydrological Processes*, *34*(7), 1514–1529. https://doi.org/10.1002/hyp.13678

Stewart, I. T., Cayan, D. R., & Dettinger, M. D. (2005). Changes toward earlier streamflow timing across western North America. *Journal of Climate*, *18*(8), 1136–1155. https://doi.org/10.1175/jcli3321.1

Stohl, A., Forster, C., & Sodemann, H. (2008). Remote sources of water vapor forming precipitation on the Norwegian west coast at 60°N-a tale of hurricanes and an atmospheric river. *Journal of Geophysical Research: Atmospheres*, *113*(D5). https://doi.org/10.1029/2007jd009006

Storey, H. C. (1955). Frozen soil and spring and winter floods. *Water. The Yearbook of Agriculture*, *1955*, 179–184.

Tarasova, L., Basso, S., & Merz, R. (2020). Transformation of generation processes from small runoff events to large floods. *Geophysical Research Letters*, *47*, e2020GL090547. https://doi.org/10.1029/2020gl090547

Tarasova, L., Basso, S., Wendi, D., Viglione, A., Kumar, R., & Merz, R. (2020). A process-based framework to characterize and classify runoff events: The event typology of Germany. *Water Resources Research*, *56*(5), e2019WR026951. https://doi.org/10.1029/2019wr026951

Tarouilly, E., Li, D., & Lettenmaier, D. P. (2021). Western U.S. Superfloods in the Recent Instrumental Record. *Water Resources Research*, *57*(9), e2020WR029287. https://doi.org/10.1029/2020wr029287

Theil, H. (1992). A rank-invariant method of linear and polynomial regression analysis. In *Henri Theil's contributions to economics and econometrics* (pp. 345–381). Springer. https://doi.org/10.1007/978-94-011-2546-8_20

Villarini, G., Serinaldi, F., Smith, J. A., & Krajewski, W. F. (2009). On the stationarity of annual flood peaks in the continental United States during the 20th century. *Water Resources Research*, *45*(8). https://doi.org/10.1029/2008wr007645

Wanders, N., Bachas, A., He, X. G., Huang, H., Koppa, A., Mekonnen, Z. T., et al. (2017). Forecasting the hydroclimatic signature of the 2015/16 El Niño event on the western United States. *Journal of Hydrometeorology*, *18*(1), 177–186. https://doi.org/10.1175/jhm-d-16-0230.1

Wasko, C., Nathan, R., & Peel, M. (2020). Trends in global flood and streamflow timing based on local water year. *Water Resources Research*, *56*(8), e2020WR027233. https://doi.org/10.1029/2020wr027233

Wasko, C., & Sharma, A. (2015). Steeper temporal distribution of rain intensity at higher temperatures within Australian storms. *Nature Geoscience*, *8*(7), 527–529. https://doi.org/10.1038/ngeo2456

Wasko, C., & Sharma, A. (2017). Global assessment of flood and storm extremes with increased temperatures. *Scientific Reports*, *7*(1). https://doi.org/10.1038/s41598-017-08481-1

Westra, S., Alexander, L. V., & Zwiers, F. W. (2013). Global increasing trends in annual maximum daily precipitation. *Journal of Climate*, *26*(11), 3904–3918. https://doi.org/10.1175/jcli-d-12-00502.1

Yan, H., Sun, N., Chen, X., & Wigmosta, M. S. (2020). Next-generation intensity-duration-frequency curves for climate-resilient infrastructure design: Advances and opportunities. *Frontiers in Water*, *2*. https://doi.org/10.3389/frwa.2020.545051

Yang, L., Smith, J., Baeck, M. L., & Morin, E. (2019). Flash flooding in arid/semiarid regions: Climatological analyses of flood-producing storms in central Arizona during the north American monsoon. *Journal of Hydrometeorology*, *20*(7), 1449–1471. https://doi.org/10.1175/jhm-d-19-0016.1

Yang, W., Yang, H., & Yang, D. (2020). Classifying floods by quantifying driver contributions in the Eastern Monsoon Region of China. *Journal of Hydrology*, *585*, 124767. https://doi.org/10.1016/j.jhydrol.2020.124767

References From the Supporting Information

Cao, Q., Mehran, A., Ralph, F. M., & Lettenmaier, D. P. (2019). The role of hydrological initial conditions on atmospheric river floods in the Russian River Basin. *Journal of Hydrometeorology*, *20*(8), 1667–1686.

Cooper, M. G., Schaperow, J. R., Cooley, S. W., Alam, S., Smith, L. C., & Lettenmaier, D. P. (2018). Climate elasticity of low flows in the maritime Western US mountains. *Water Resources Research*, *54*(8), 5602–5619. https://doi.org/10.1029/2018wr022816

Helsel, D. R., Hirsch, R. M., Ryberg, K. R., Archfield, S. A., & Gilroy, E. J. (2020). *Statistical methods in water resources*. US Geological Survey. https://pubs.er.usgs.gov/publication/tm4A3

Lettenmaier, D. P. (1976). Detection of trends in water quality data from records with dependent observations. *Water Resources Research*, *12*(5), 1037–1046.

Lettenmaier, D. P., Wood, E. F., & Wallis, J. R. (1994). Hydro-climatological trends in the continental United States, 1948-88. *Journal of Climate*, *7*(4), 586–607.